FT-Raman, FT-IR and NMR spectra, vibrational assignments and density functional studies of 1,3-bis(benzimidazol-2-yl)-2-thiapropane ligand and its Zn(II) halide complexes

ARTICLE *in* STRUCTURAL CHEMISTRY · FEBRUARY 2007

Impact Factor: 1.84 · DOI: 10.1007/s11224-007-9238-y

Struct Chem (2008) 19:21–32
DOI 10.1007/s11224-007-9238-y

ORIGINAL PAPER

FT-Raman, FT-IR and NMR spectra, vibrational assignments and density functional studies of 1,3-bis(benzimidazol-2-yl)-2-thiapropane ligand and its Zn(II) halide complexes

Naz Mohammed Aghatabay · Metin Tulu · Mehmet Somer · Durata Haciu · Ayberk Yilmaz

Received: 24 May 2007 / Accepted: 29 August 2007 / Published online: 29 September 2007

Abstract 1,3-bis(benzimidazol-2-yl)-2-thiapropane (L) ligand and its zinc halide ZnX_2 (X = Cl, Br, I) complexes have been synthesized. The compounds were characterized using the elemental analysis, molar conductivity, FT-Raman, FT-IR (mid i.r., far i.r.), ^1H and ^{13}C NMR spectra, and quantum chemical calculations performed with Gaussian 03 package program set. The optimized geometries and vibrational frequencies of the ligand and $[Zn(L)Cl_2]$ complex were calculated using the DFT/B3LYP method with a 6–31g(d) basis set. The geometry optimization of $[Zn(L)Cl_2]$ yields a slightly distorted tetrahedral environment around Zn ion, while the molecule clearly reveals the Cs symmetry. The molar conductivity data reveals that the complexes are neutral. The ligand is bidentate, via two of the imine nitrogen atoms in the bis-imidazole ring units, and together with the monodentate coordination of the two halides to the metal centre.

Keywords Benzimidazole · Bidentate · Distorted · Mononuclear · Quantum chemical calculations · Tetrahedral

N. M. Aghatabay (✉) · M. Tulu
Department of Chemistry, Fatih University, Büyükçekmece, Istanbul 34500, Turkey
e-mail: natabay@fatih.edu.tr; natabay@yahoo.com

M. Somer · D. Haciu
Department of Chemistry, Koç University, Rumelifeneri Yolu, Sariyer, Istanbul 34450, Turkey

A. Yilmaz
Department of Physics, Istanbul University, Vezneciler, Istanbul 34459, Turkey

Introduction

Due to structural similarities with the common purine type nucleobases, the bis-benzimidazole derivatives, together with their transition metal complexes have attracted a great deal of interest in coordination and medicinal chemistry [1–8]. In addition to their biological importance, these ligands are strongly coordinating agents and form stable complexes with various transition metal ions. Among the transition metal complexes, the interest in Zn(II) and its analogue complexes containing N and S donor ligands has increased in recent years [9, 10]. Coordination numbers of Zn(II) are most commonly four to six, with adoptions of a variety of distorted coordination geometries without significant energy penalty. Depending on donor or ligand types, distorted tetrahedral, square planar, five-coordinate geometries and octahedral are frequently observed geometries. The coordinating environment provided by the thioether-bridging ligand **(L)** and its several species with various transition metal ions, including Zn^{2+} have been previously examined crystallographically [11, 12]. In the solid state, thioether ligand provided the expected N_2 donor set from the tertiary imine nitrogen atoms forming preferred four-co-ordinate tetrahedral environment, and the remaining coordination sites were filled by halide anions [12]. Metal ion selectivity and transportation ability of several bis(benzimidazloe) ligands have also been studied in terms of the condition (pH), bridge length, donating atom (hard-soft principle) and the geometrical constrains provided by the ligands [13]

Although the spectroscopic studies, particularly on the vibrational frequencies of the bis-benzimidazole derivatives and some metal(II) halide complexes have been previously reported. Theoretical prediction of vibrational spectra is of practical importance for characterization of

chemical compounds, and has become an important part of spectra-chemical and quantum investigations. There has been no complete study and assignment on the spectroscopic and magnetic properties of these compounds. Hence, investigations on the structures of the ligands and related metal complexes are very important for better understanding of their molecular properties. The aim of the present work is, by using a wide range of spectroscopic methods, together with quantum calculations, characterize the 1,3-bis(benzimidazole-2-yl)-2-thiapropane (L) ligand and its Zn(II) halide complexes. In this respect a detailed quantum chemical study will aid in making definitive assignments to the fundamental modes observed in the FT-IR and FT-Raman spectra, which are calculated for the ligand (L) and the $[Zn(L)Cl_2]$ complex, based on the total energy distribution (TED). Because of the structural analogy the results are directly transferred to the bromo and iodo complexes as well.

Experimental

Materials and methods

Apart from *o*-phenylenediamine (freshly sublimed), all other starting compounds and solvents were used as commercial products of analytical grade without any purification. The ligand (L) was prepared by literature procedures [14–16]. Molar conductivity of the complexes was measured on a WPA CMD750 conductivity meter in dimethyl sulfoxide (DMSO) solution at 25 °C. FT-IR spectra were recorded as KBr pellets (mid, 4,000–400 cm^{-1}) and in polyethylene discs (far, 600–175 cm^{-1}) on a Jasco FT/IR-600 Plus Spectrometer. Raman spectra were obtained from powdered samples placed in a Pyrex tube using a Bruker RFS 100/S Raman spectrometer in the range 4,000–0 cm^{-1}. The 1,064 nm line, provided by a near infrared Nd:YAG air-cooled laser was used as excitation line. The output laser power was set to 100–120 mW. Routine ^1H and ^{13}C NMR spectra were recorded at ambient temperature, on a 500 MHz NMR Spectrometer in DMSO-d_6. Chemical shifts (δ) are expressed in units of ppm relative to tetramethylsilane.

Synthesis

1,3-bis (benzimidazol-2-yl)-2-thiapropane (L) [14–16]

To a mixture of 2,2′-thiodiethanoic acid (2.0 g, 13.3 mmol) and freshly sublimed *o*-phenylenediamine (3.63 g, 26.7 mmol) was added in 5 M HCl (30 cm^3). The mixture was refluxed for 24 h. The precipitates were collected and

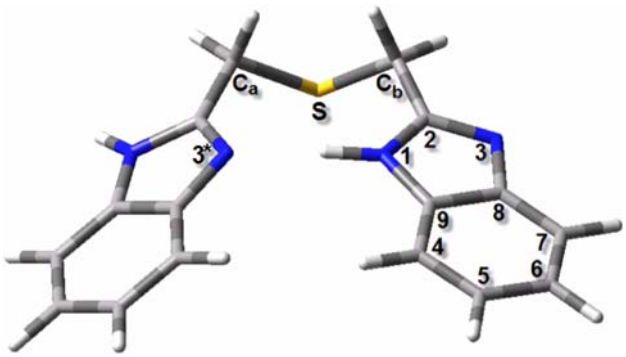

Fig. 1 Optimised structure of the ligand (**L**)

treated with an aqueous ammonia solution (m.p. 221 °C). ^1H-n.m.r. (500 MHz): δ_H 3.85 (4H, s, CH_2), 6.96 (4H, s, H_5 and H_6), 7.32 (4H, s, H_4 and H_7), (2H, NH not detected); $^{13}C\{^1H\}$-n.m.r. (125 MHz): δ_C 29.04 (2C, CH_2), 115.17 (4C, C_4 and C_7), 122.19 (4C, C_5 and C_6), 138.93 (4C, C_8 and C_9), 152.10 (2C, C_2). The Raman and i.r. frequencies and their assignments are presented in Table 1.

[Zn(L)Cl$_2$] complex

A solutions of (L) (100 mg, 0.34 mmol) and $ZnCl_2$ (48 mg, 0.35 mmol) in absolute EtOH (8 cm^3) were refluxed overnight. The white solid was collected, and washed several times with small portions of cold ethanol to make it pure (113 mg, 65%). Dec. >300 °C. (Found: C, 44.2; H, 3.5; N, 12.8 $C_{16}H_{14}Cl_2N_4SZn$ calcd: C, 44.7; H, 3.3; N, 13.0%). ^1H-n.m.r. (500 MHz): δ_H 4.06 (4H, s, CH_2), 7.39 (4H, s, H_5 and H_6), 7.68 (2H, s, H_7), 8.29 (2H, s, H_4), 13.68 (2H, s, NH); $^{13}C\{^1H\}$-n.m.r. (125 MHz): δ_C 25.17 (2C, CH_2), 112.25 (2C, C_7), 118.05 (2C, C_4), 123.85 (2C, C_6), 124.25 (2C, C_5), 132.36 (2C, C_8), 139.10, (2C, C_9), 151.95 (2C, C_2). The molar conductivity was 7.1 $\Omega^{-1}cm^2mol^{-1}$. The Raman and i.r. frequencies and their assignments are listed in Table 2.

[Zn(L)Br$_2$] complex

This white crystalline complex was prepared in a manner similar to that employed for $Zn(L)Cl_2$ complex using a mixture of (L) (100 mg, 0.34 mmol) and $ZnBr_2$ (78 mg, 0.35 mmol) in absolute EtOH (6 cm^3). The yield was (120 mg, 68%). Dec. >300 °C. (Found: C, 36.8; H, 2.9; N, 10.7. $C_{16}H_{14}Br_2N_4SZn$ calcd: C, 37.0; H, 2.7; N, 10.8%). ^1H-n.m.r. (500 MHz): δ_H 4.02 (4H, s, CH_2), 7.40 (4H, s, H_5 and H_6), 7.70 (2H, s, H_7), 8.28 (2H, s, H_4), 13.68 (2H, s, NH); $^{13}C\{^1H\}$-n.m.r. (125 MHz): δ_C 25.11 (2C, CH_2), 112.30 (2C, C_7), 118.10 (2C, C_4), 123.65 (2C, C_6), 124.15

Table 1 Experimental and computed vibrational frequency data of the ligand (L) in the 3,500-10 region cm^{-1}

MN	IR	Raman	Scale[a]	TED (phases and %)[b]
Q1	3365sh		3509	ν(N–H)(100)
Q2	3143b		3246	ν(C–H)(99)
Q3	3085b		3096	ν(C–H)(99)
Q4			3092	ν(C–H)(99)
Q5			3088	ν(C–H)(100)
Q6	3062b	3069	3078	ν(C–H)(100)
Q7		3057	3071	ν(C–H)(100)
Q8	3017b		3061	ν(C–H)(100)
Q9	2936b	2975	3034	$\nu(CH_2)$(100)
Q10			3019	$\nu(CH_2)$(100)
Q11			2966	$\nu(CH_2)$(100)
Q12			2956	$\nu(CH_2)$(100)
Q13	1624m	1626w	1648	ν(C–C)(6mr)(55), ν(C–N)(5mr)(14)
Q14			1646	ν(C–C)(6mr)(57), ν(5mr)(13), δ(CH)(11)
Q15	1590w	1594ms	1609	ν(C–C)(6mr)(52),ν(C–C)(19), δ(CH)(12)
Q16			1606	ν(C–C)(6mr)(51), ν(C–C)(17), δ(CH)(12)
Q17	1535ms	1536vs	1556	ν(5mr)(29), δ(NH)(24), ν(C–C) (6mr)(19)
Q18			1544	ν(5mr)(44), ν(6mr)(14), ν(C–C)(13), δ(NH)(11)
Q19	1490w	1490m	1508	ν(6mr)(33), δ(CH)(28), ν(5mr)(21)
Q20			1506	ν(6mr)(33), δ(CH)(27), ν(5mr)(22)
Q21			1471	δ(CH)(31), ν(5mr)(24), ν(6mr)(13)
Q22			1465	δ(CH)(43), ν(C–C)(17), (6mr)(16) ν(5mr)(16)
Q23	1443vs	1452s	1454	$sc(CH_2)$(77)
Q24		1444s	1437	$sc(CH_2)$(75), ν(5mr)(12)
Q25	1421sh	1422sh	1431	ν(5mr)(31), $sc(CH_2)$(16), δ(NH) (15),δ(CH)(15)
Q26	1383sh	1384m	1393	ν(6mr)(34), ν(5mr)(19), δ(CH)(17)
Q27			1383	ν(6mr)(46), δ(CH)(16), ν(5mr)(13)
Q28		1367sh	1324	δ(CH)(28), ν(6mr)(24), ν(5mr)(22)
Q29	1314m	1313w	1319	δ(CH)(4), ν(5mr)(21), ν(6mr)(17)
Q30			1286	ν(5mr)(30), δ(CH)(23), ν(6mr)(18)
Q31			1281	ν(5mr)(43), ν(6mr)(21), δ(CH)(23)
Q32	1272vs	1270vs	1273	$\omega(CH_2)$(68), δ(CH)(13)
Q33			1254	$\omega(CH_2)$(80)
Q34		1239m	1237	δ(CH)(32), ν(5mr)(21), ν(6mr)(17),δ(NH)(13)
Q35			1227	ν(5mr)(37), δ(CH)(21), δ(NH)(18), ν(6mr)(12)
Q36	1225s	1225	1213	ν(5mr)(23), $t(CH_2)$(22), δ(NH)(21),ν(6mr)(13)
Q37			1172	$t(CH_2)$(69), ν(5mr)(12)
Q38	1158s	1152m	1161	δ(CH)(77), ν(6mr)(16)
Q39			1157	δ(CH)(78), ν(6mr)(16)
Q40	1127s	1116m	1138	$t(CH_2)$(63), ν(5mr)(13)
Q41			1121	δ(CH)(48), ν(6mr)(34)
Q42	1026s	1027s	1025	ν(6mr)(44), δ(CH)(17), ν(5mr)(16), δ(5mr)(16)
Q43			1021	ν(6mr)(52), δ(CH)(21), ν(5mr)(11), δ(5mr)(11)
Q44	1000sh	1001m	1004	ν(6mr)(29), ν(5mr)(23), δ(5mr)(21)
Q45			997	ν(5mr)(28), δ(5mr)(23), ν(6mr)(21),ν(C–C)(12)
Q46	928m	927vw	956	γ(CH)(100)
Q47			950	γ(CH)(100)
Q48			915	$\rho(CH_2)$(38), ν(6mr)(27), ν(5mr)(12)
Q49	906vw	886w	912	γ(CH)(100)
Q50			908	γ(CH)(100)
Q51	865s		897	ν(6mr)(61), ν(5mr)(16)
Q52			878	ν(6mr)(40), $\rho(CH_2)$(33), ν(5mr)(12)

Table 1 continued

MN	IR	Raman	Scale[a]	TED (phases and %)[b]
Q53	847s	846s	846	γ(CH)(47), ν(6mr)(12), ν(C–C)(11)
Q54			845	γ(CH)(45), ν(6mr)(12), ν(C–C)(11)
Q55			843	ν(6mr)(24), ν(C–C)(24), γ(CH)(15),ν (5mr)(12)
Q56			842	γ(CH)(78)
Q57	816m		819	$\rho(CH_2)$(67)
Q58			781	δ(NH)(61), ν(5mr)(24)
Q59		766sh, 751m	762	τ(6mr)(50), τ(5mr)(36), γ(CH)(11)
Q60			760	τ(6mr)(43), τ(5mr)(35), γ(CH)(12)
Q61			749	τ(5mr)(27), γ(CH)(24), γ(C–C)(17), τ(6mr)(12),
Q62	735vs	736m, 720m	742	γ(CH)(77)
Q63			738	γ(CH)(64)
Q64			714	ν(CS)(28), γ(NH)(18), γ(C–C)(14), δ(CSC)(12)
Q65	641w 623vw	632s	710	δ(6mr)(19), δ(5mr) (18), ν(CS)(15), γ(C–C)(12)
Q66			701	ν(CS)(31), δ(6mr)(18), δ(5mr) (16),γ(C–C)(12)
Q67			629	τ(5mr)(26), ν(CS)(25), δ(6mr)(21)
Q68			620	δ(5mr)(41), δ(6mr)(34), ν(6mr)(21)
Q69			616	δ(5mr)(42), δ(6mr)(31), ν(6mr)(21)
Q70	612vw		612	ν(CS)(34), τ(5mr)(25), δ(6mr)(14)
Q71	577w	578w	577	τ(6mr)(78), τ(5mr)(22)
Q72			576	τ(6mr)(77), τ(5mr)(23)
Q73	530w	516m	515	δ(6mr)(43), ν(5mr)(12), ν(6mr)(12)
Q74	506s		513	δ(6mr)(43), ν(5mr)(13), ν(6mr)(12)
Q75	477m		469	δ(6mr)(38), δ(CC)(25), δ(5mr)(13)
Q76			462	γ(NH)(41), δ(6mr)(24), δ(CC)(13)
Q77	456w		456	γ(NH)(56), δ(6mr)(17)
Q78	438s	439w	435	τ(6mr)(65), but(CC)(22)
Q79			434	τ(6mr)(69), but(CC)(19)
Q80	361s	360m	351	τ(6mr)(29), δ(CSC)(13), ν(CS)(11)
Q81	352w		342	τ(6mr)(32), γ(CC)(15), δ(CSC)(11)
Q82	306		314	δ(CSC)(32), δ(CC)(14)
Q83	278sh	279vw	263	τ(6mr)(64), τ(5mr)(30)
Q84	270		260	τ(6mr)(64), τ(5mr)(30)
Q85	218s		254	δ(CC)(43), τ(6mr)(17), ν(5mr)(12)
Q86	204m		199	δ(CSC)(24), but(CC)(22), δ(CC)(12)
Q87	197m, 187m	152s	184	δ(CSC)(32), but(CC)(25)
Q88			168	δ(CSC)(40), ν(CS)(16)
Q89		102vs	94	τ(CS)(27), γ(CC)(25), τ(SC)(23)
Q90		84vs	72	τ(SC)(40), τ(CC)(16), γ(CC)(15)
Q91			60	τ(CC)(60)
Q92			58	τ(CC)(40), γ(CC)(17)
Q93		38s	32	τ(SC)(54), τ(CS)(24), γ(CC)(21)
Q94			16	τ(CS)(41), τ(CC)(30)

[a] Modes Q1–Q12 were scaled by 0.9620, Q13–Q70 by 0.980 and Q71–Q 94 not scaled, see text

[b] Vibrational assignment is based on the calculated total energy distribution (TED), only contributions over 10% are listed. ν, stretching; δ, in-plane bending; γ, out-of-plane bending; τ, torsion; ρ, rocking; t, twisting; ω, wagging; but, butterfly; sc, scissoring; 6-membered ring (6mr), 5-membered ring (5mr)

(2C, C_5), 132.85 (2C, C_8), 139.0, (2C, C_9), 151.80 (2C, C_2); Mid-i.r.: ν_{max}/cm^{-1} includes; 3325 ν(N–H), 1623 ν(C–C), 1595 ν(C=N), 1451 ν(C=N), 1279 ν(C–C), 748γ(C–H); Far-i.r. 512, 438, 360, 302, 288 ν(Zn–Br), 253 ν(Zn–N), 198 ν(Zn–N); Raman: ν_{max}/cm^{-1} 3074 ν(C–H), 3070 ν(C–H), 2940 (CH_2), 2927 $\nu(CH_2)$, 1622 ν(C–C), 1595 ν(C=N),

1529sc(CH_2), 1451 ν(C=N), 1281 ν(C–C), 1,252, 760 γ(C–H), 518, 488 δ(6mr), 440, 365, 321new, 287 ν(Zn–Br), 251 ν(Zn–N), 218 ν(Zn–Br), 180 ν(Zn–N), 143, 107, 88, 57, 72, 57. The molar conductivity was 6.5 $\Omega^{-1}cm^2mol^{-1}$.

[Zn(L)I_2] complex

This white solid complex was prepared in a manner similar to that used for [Zn(L)I_2] reacting a mixture of (L) (100 mg, 0.34 mmol) and ZnI_2 (110 mg, 0.35 mmol) in absolute EtOH (6 mL). The yield was (132 mg, 63%). Dec. >300 °C. (Found: C, 30.9; H, 2.5; N, 8.8. $C_{16}H_{14}Cl_2N_4SZn$ calcd: C, 31.3; H, 2.3; N, 9.1%). ^{1}H-n.m.r. (500 MHz): δ_H 4.10 (4H, s, CH_2), 7.3.95 (4H, s, H_5 and H_6), 7.83 (4H, s, H_4 and H_7), 13.80 (2H, br, NH); $^{13}C\{^1H\}$-n.m.r. (125 MHz): δ_C 25.10 (2C, CH_2), 112.45 (2C, C_7), 118.25 (2C, C_4), 123.75 (2C, C_6), 124.18 (2C, C_5), 132.93 (2C, C_8), 139.20, (2C, C_9), 151.78 (2C, C_2); Mid-i.r.: ν_{max}/cm^{-1} includes; 3329 ν(N–H), 3104 ν(C–H), 3073 ν(C–H), 2958 ν(CH_2), 2937 ν(CH_2), 1623 ν(C-C), 1595 ν(C=N), 1448, 1278 ν(C–C), 750 γ(C-H); Far-i.r.: 512, 487, 437, 359, 303, 288 (Zn–N), 250 (Zn–I), 209 (Zn–N), 201, 183; Raman: ν_{max}/cm^{-1} 3067 ν(C–H), 2970 ν(CH_2), 2938 ν(CH_2), 2924ν(CH_2), 1622 ν(C–C), 1595 ν(C=N), 1448, 1278 ν(C–C), 750 γ (C–H), 518, 488, 440, 365, 288 (Zn–N), 248 (Zn–I), 201 (Zn–N), 180, 160 (Zn–I), 132, 116, 97, 77, 40. The molar conductivity was 8.7 $\Omega^{-1}cm^2mol^{-1}$.

Theoretical calculations

The computational calculations were performed with the Gaussian 03 package program set [17]. The optimized geometries and vibrational wavenumbers of both ligand and the [Zn(L)Cl_2] complex were calculated using the DFT/B3LYP method with a 6–31g(d) basis set (Figs. 1, 2). The geometry optimization of [Zn(L)Cl_2] complex yields a slightly distorted tetrahedral environment around Zn. Comparison of the calculated values (for the complex) of bond lengths d(N–Zn–N), d(Cl–Zn–Cl) and bond angles ∠N−Zn−N,∠Cl−Zn−Cl with experimental values that were reported previously do indicate only marginal differences [12]. The calculated (experimental) values are: bond lengths d(N–Zn–N), 2.080 (2.045–2.008); d(Cl–Zn–Cl), 2.2737–2.2377 (2.2487–2.2621) Å; and bond angles ∠N−Zn−N, 107.082 (107.7); ∠Cl−Zn−Cl, 112.7 (112.26°), ∠Cl−Zn−N, 112.033–108.771, while the molecule clearly reveals the Cs symmetry (Fig. 2). The calculated (C–S) bond lengths for the complex and free ligand are directly comparable: d(S–C–S), 1.8541 (complex) and d(C–S–C), 1.857–1.853 Å ligand, respectively. Also the deviation in the bond angles (C_a–S–C_b) is only marginal: 102.145° (complex), ∠C−S−C = 102.331 (ligand).

The assignment of the Raman and i.r. active vibrational modes was supported by total energy distribution (TED), performed with the SCALE2 program [18]. The non-redundant sets of 94 and 101 normal modes of internal vibrations has been defined as recommended by Pulay et al. for the ligand and [Zn(L)Cl_2] complex, respectively [19]. Each of the vibrational modes was assigned to one of the nine types of motion predicted by the point group analysis: stretching, in-plane bending, out-of-plane bending, torsion, rocking, twisting, wagging, scissoring, butterfly.

The calculated frequencies are usually slightly higher than the observed values for the majority of the normal modes, particularly in the higher frequency regions. Two major factors may be responsible for the discrepancies between the experimental and computed values are the environmental phase value (solid–gas) and the anharmonic–harmonic frequency. For these reasons, interpretation of experimental data usually requires theoretical frequencies to be scaled: high frequency modes with a smaller factor (by ca. 0.96) and the low frequency modes with a factor close to 1 [20] or by using a linear regression fitting [21]. In order to decrease overestimation of the calculated vibrational frequencies, the obtained values were scaled by 0.9620 at higher frequencies taken for DFT/B3LYP method with a 6–31g(d) basis set from Standard Reference Database and by 0.980 factors for middle frequencies [22]. No escalation was required for the lower frequencies. The computational and experimental data for both Raman and FT-IR spectra, together with TED values were given in Tables 1 and 2 for the ligand and [Zn(L)Cl_2] complex. In order to be able to compare the experimental and calculated spectra visually, the

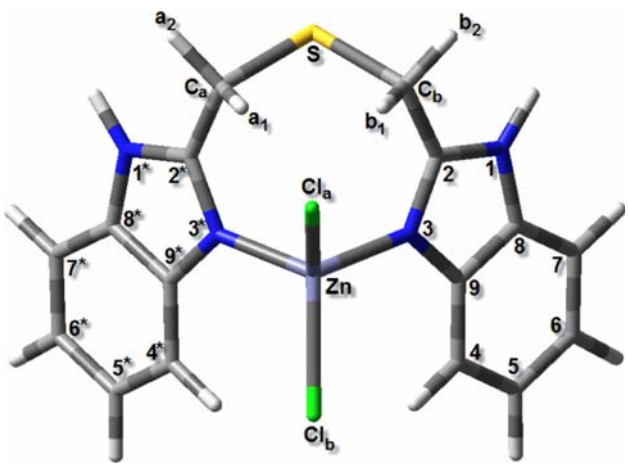

Fig. 2 Optimised structure of the Zn(L)Cl_2 complex

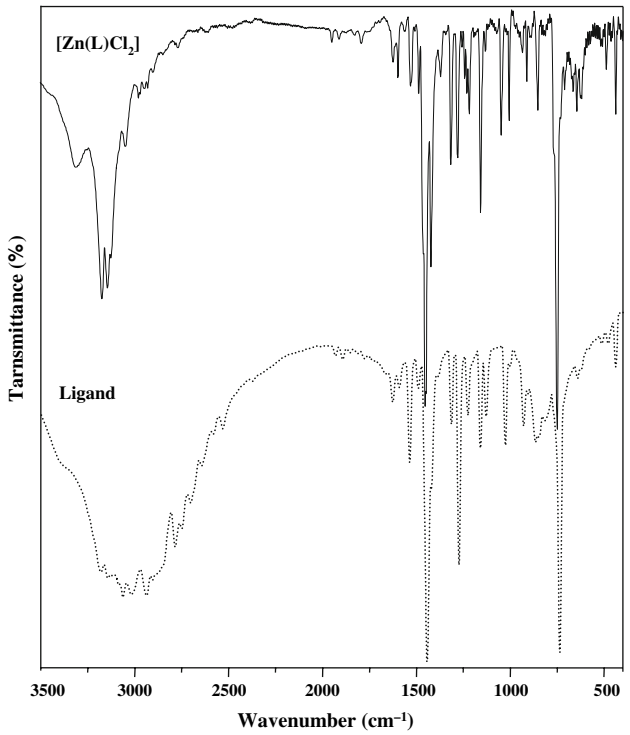

Fig. 3 FT-IR spectrum of (L) and $[Zn(L)Cl_2]$ in the 3,500–400 cm^{-1} region

theoretical data were stimulated using the frequencies and Raman scattering activities calculated by all methods assuming Lorentzian band shapes having a band width of 7 cm^{-1}.

Results and discussion

Infrared and Raman spectra

In Tables 1 and 2 are gathered the observed and calculated (scaled) vibrational wavenumbers of the Raman and FT-IR with a detailed description of the normal modes based on the TED. The stimulated Raman and IR spectra closely resemble the observed spectra and it is particularly impressive when one takes into account that they are the spectrum of the solid compound. Although there are some differences in the calculated versus experimental, these data demonstrate the utility of ab initio calculations in predicting the vibrational assignments for these types of big molecules.

The assignment of the vibrational frequencies for the complex series $[Zn(L)X_2]$ (X = Cl, Br, I) is only calculated for $[Zn(L)Cl_2]$ complex, because of the structural analogy, the results are directly transferred to the bromo and iodo complexes. Significant differences are expected only in the low frequency region, which is characteristic for the zinc-halide and zinc-nitrogen stretching and deformation modes [23, 24]. In accordance with the predictions the similarity between the vibrational spectra of the $[Zn(L)X_2]$ complexes (X = Cl, Br, I) concerning the wave-numbers of the modes $\nu > 800$ cm^{-1} and their band intensities is very marked. As revealed by TED, one (Q1) and two (Q1, Q2) pure modes are associated with the N–H stretching of imine group for the ligand and the $[Zn(L)Cl_2]$ complex, respectively. An unresolved shoulder at 3,365 cm^{-1} in i.r. spectrum of the ligand could be assignable to ν(N–H). The broadness may have caused due to the fluxional behaviour of the imine hydrogen atoms and internal hydrogen bonding. These bands appear in all three complexes as a broad medium band at ca. 3,300 cm^{-1} (Fig. 3). This supports the contention that coordination may occur through both bis-3 and 3′ nitrogen atoms, causing inhibition of the fluxional behaviour of the imine hydrogen atoms. In the Raman spectra these modes are too weak to be observed.

According to TED, the pure characteristic ν(C–H) modes of ring residues and aliphatic groups are observed in the wave regions 3,116–2,954 cm^{-1}, having 6 and 4 modes respectively, both for the ligand and the complex. These bands are observed both in i.r. and Raman for the ligand and the complexes as predicted. Slight but specific differences between spectra of the free ligand and the complexes in this region support for the formation of new complexes particularly on the ν(CH) modes of ring residues (Figs. 3, 4).

As revealed by TED and as expected, specific differences are observed for the C–C aromatic semicircle stretching vibrations of the ligand and the complex. In the free ligand several modes are associated with ν(C–C) vibrations. These stretches are combined with a strong contribution from the δ(N–H), δ(C–H) and ν(C–N) vibrations. As in the $[Zn(L)Cl_2]$ complex, the ν(C–C) vibrations are more characteristic and pure, may be due to prohibition of the fluxional behaviour of the imine hydrogen atoms via nitrogen complexion (Q13–14). In this respect the frequencies values are in good agreements between the experimental and computed frequencies for the ligand and complexes, these bands are appeared at ca. 1,620 both in i.r. and Raman spectra and supported by the literature data. Similarly, the ν_{as}(C=N) frequencies are expected to appear around 1,600 cm^{-1}. Thus, qualitatively, the i.r. band at 1,590 cm^{-1} in the free ligand shifts to 1,596, 1,595, 1,595 cm^{-1} for the $[Zn(L)Cl_2]$, $[Zn(L)Br_2]$ and $[Zn(L)I_2]$, respectively. These frequencies could represent the respective ν(C=N) mode. However, the TED values in Table 2 reveal that this mode is not characteristic and is strongly coupled with several vibrations, including δ(C–H), δ(N–H) and ν(C–C) vibrations (modes 16 and 17). In the free ligand these particular modes are dominated only by C–H aromatic in-plane bending and C–C stretching vibrations (modes 15, 16).

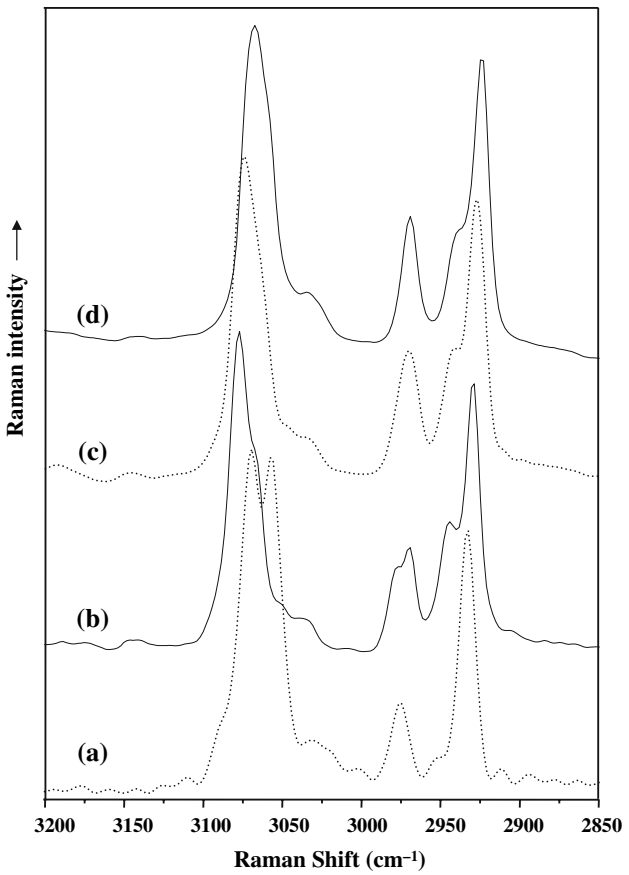

Fig. 4 Raman spectrum of (**a**) ligand, (**b**) $[Zn(L)Cl_2]$, (**c**) $[Zn(L)Br_2]$, (**d**) $[Zn(L)I_2]$ in the 3,200–2,850 cm^{-1} region

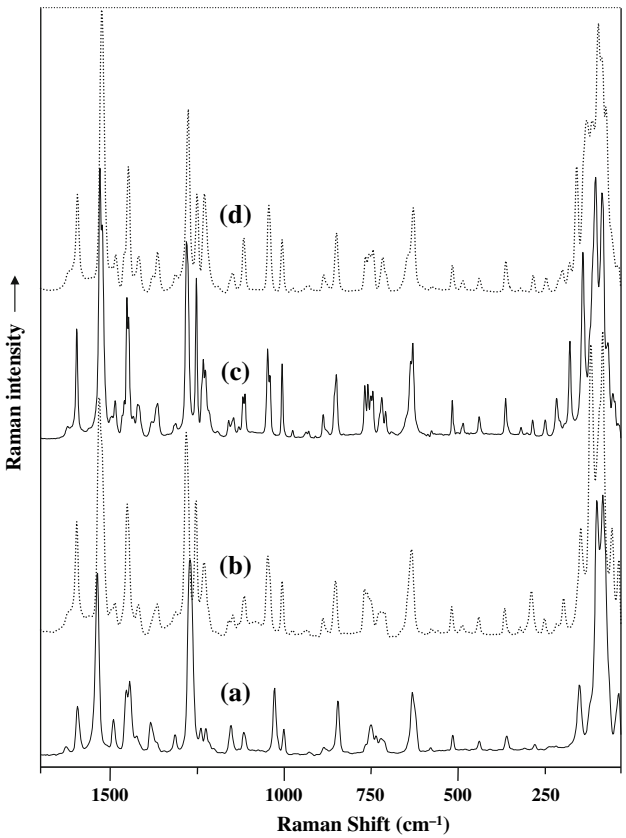

Fig. 5 Raman spectrum of (**a**) ligand, (**b**) $[Zn(L)Cl_2]$, (**c**) $[Zn(L)Br_2]$, (**d**) $[Zn(L)I_2]$ in the 1,700–32 cm^{-1} region

In accordance with TED, the strong bands at 1,452 and 1,444 cm^{-1} (modes 23–25) in Raman and a very strong band at 1,443 cm^{-1} in i.r. spectrum corresponds to CH_2 scissoring vibrations for the free ligand. This is almost pure mode as evidenced from 83% and 75% of TED (Table 1). In complexation CH_2 scissoring vibrations appear at 1,460, 1,452 in Raman and 1,452 cm^{-1} in i.r. spectrum (Table 2). Strong bands at 1,421 cm^{-1} in both Raman and i.r. are clearly assignable to ν_s(C=N) frequencies of the coordinated ligand, through its imine nitrogen atoms (Table 2, Q26). The mode Q32 in the complex is dominated by $\omega(CH_2, 90\%)$ vibration at 1,271 cm^{-1}, which appears as a strong band at 1,278 and 1,279 cm^{-1}in Raman and i.r. spectrum, respectively (Figs. 3, 5). These assignments are in agreement with the literature data [25, 26].

In the middle frequency region for both the ligand and the complex are dominated by (CH_2) wagging, (C–H) in-plane bending, (CH_2) torsion and ring stretching vibrations. These wavenumbers are in reasonable agreement with experimental results (See "Experimental" and Tables 1, 2).

Out of particular interest is the lower frequency region, characteristic for the ν(Zn–N) and ν(Zn–X) (X = Cl, Br, I) modes. The anhydrous zinc halides ZnX_2 (X = Cl, Br, I) show strong Raman bands at 228, 161 and 121 cm^{-1}, respectively (Fig. 6). However, the position of the fourfold coordinating halogen atoms in these salts is only bridging while in the title compounds both are terminal. More realistic for comparison are therefore the infrared vibration values of the (ν_{as}) and (ν_s) for (Zn–X)-stretches taken from the tetrahedral anionic series $[ZnX_4]^{2-}$ (X = Cl, Br, I); (ν_{as})/(ν_s): 294/279 (Cl), 207/172 (Br) and 122/170 (I) cm^{-1} [27]. The vibrational values of the tetrahedral tetra-halo anions, such as $(Et_4N)_2ZnX_2$ in the solid state in which the tetrahedral geometry of the anion is retained for the corresponding quaternary ammonium halides, are also more realistic values for comparison. The ν(Zn–X) frequency values within the series of $(Et_4N)_2ZnX_2$: Raman/IR are 276/277 (Cl), 171/207 (Br) and 118/165 cm^{-1} [28]. Even more realistic values may be obtained from the vibration values of the tetrahedral series $[Zn(pyridine)_2X_2]$, for the i.r. spectra values: (X = Cl, Br, I); (ν_{as})/ (ν_s): 327/295 (Cl), 260/213 (Br) and 221/147 cm^{-1} and the bands at 200 150, 140 and 102 cm^{-1} remain for assignment to the four possible combination vibrations of δ[X–Zn–N] bending modes in the Raman spectra [29].

According to TED, the $[Zn(L)Cl_2]$ complex predicts for ν_{as}(Zn–Cl) and ν_s(Zn–Cl) two bands at 320 (Q_{81}, 93%) and

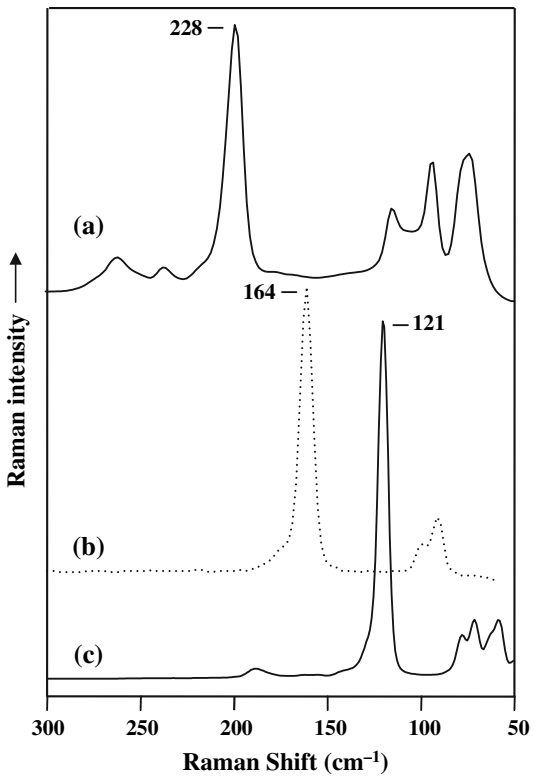

Fig. 6 The 300–50 cm^{-1} region Raman spectrum of (**a**) $ZnCl_2$, (**b**) $ZnBr_2$ and (**c**) ZnI_2

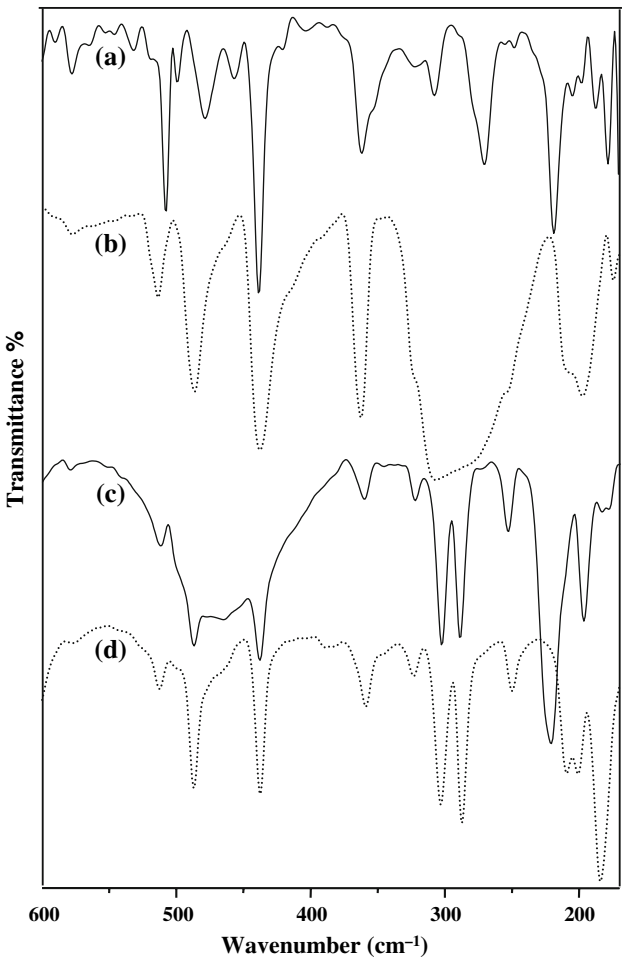

Fig. 7 The 600–170 cm^{-1} region FT-IR spectrum of (**a**) (L), (**b**) $[Zn(L)Cl_2]$, (**c**) $[Zn(L)Br_2]$, and (**d**) $[Zn(L)I_2]$

285 cm^{-1} (Q_{84}, 93%), respectively. The far-IR spectra (Fig. 7) show that all three complexes vibrate moderately in this region. The $[Zn(L)X_2]$ complex exhibit bands at 340–250 broad (320, 307) (X = Cl); 288, 221 (X = Br) and 248 cm^{-1} (X = I), arising from the antisymmetric and symmetric metal–halogen stretches. Similarly the complexes exhibit absorptions in the Raman spectra at 323 and 290 (Cl); 288, 219 (Br) and 202 and 160 cm^{-1} (I), respectively. The increase for the ν(Zn–Cl) in $[Zn(L)Cl_2]$ with respect to $[ZnCl_4]^{2-}$ is due to the lack of the negative charges which weakens the bond as a rule. The broadness for ν(Zn–Cl) modes in i.r. spectrum probably caused by doubly intramolecular hydrogen bonding between a strong electronegative element chloride ion and one of the hydrogen atom of the benzimidazole ring, namely H_4 and $H_{4'}$, which is also the case for proton nmr.

Based on the vibrational spectroscopical data for the different Zn–pyridine [30, 31] and Zn–amino complexes [32], both antisymmetric and symmetric vibration of Zn–N is expected to appear at 300–200 cm^{-1} region. In the title compounds the nitrogen ligands are not "free" but integrated in an 8-membered chelate ring (Fig. 2). Indeed, the TED values for ν(Zn–N) in $[Zn(L)Cl_2]$ at 237, 201, 188 and 176 cm^{-1} (modes 86–89) clearly indicate that these vibrations are not characteristic and strongly mixed with the modes from the chelate ring. The bands at 240vb, 197, in i.r. and 215, 196 cm^{-1} in Raman spectra may be assignable for these two vibration modes, respectively. Similar values are expected also for the $[Zn(L)Br_2]$ and $[Zn(L)I_2]$ complexes, since the effect of the halides will be small on ν(Zn–N) vibrations (Fig. 7, 8).

According to TED, the Raman spectrum of the ligand at the lower frequency region is dominated by deformation modes, such as δ(CSC), τ(C–S) and τ(C–C), while in the $[Zn(L)Cl_2]$ complex, the dominant deformation vibrations are appeared to be the chelating rings and zinc-halides (Tables 1, 2).

Nuclear magnetic resonance

In the free ligand, the aromatic protons are observed as slightly broad singlets at δ 6.96 and 7.32 ppm, corresponding to the two sets of H(4, 7) and H(5, 6) protons, respectively. The bridging CH_2 proton is observed as a

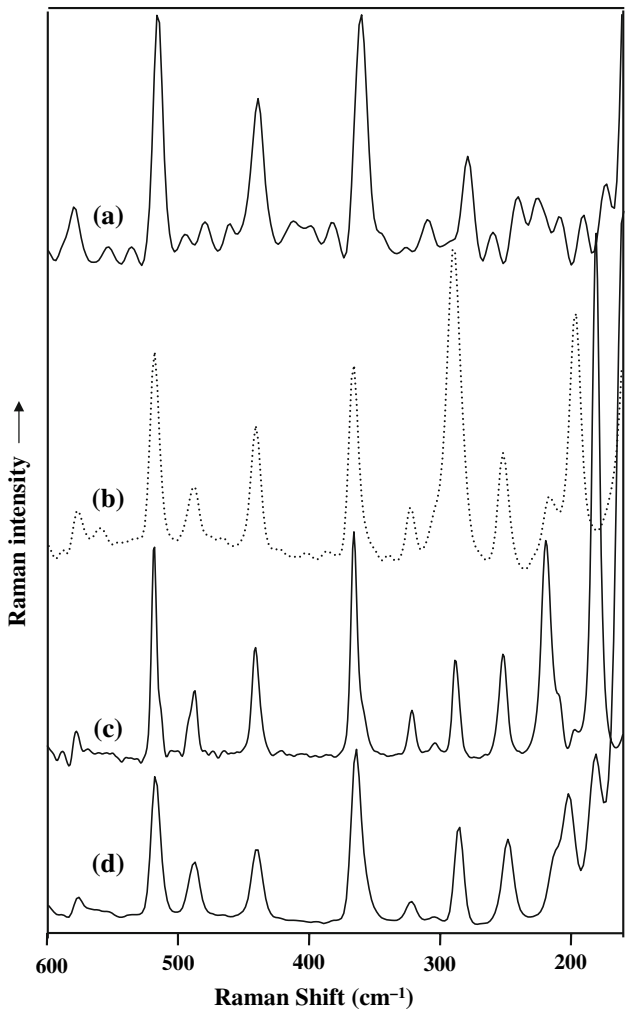

Fig. 8 The 600–160 cm^{-1} region Raman spectra of (**a**) (L), (**b**) $[Zn(L)I_2]$, (**c**) $[Zn(L)Br_2]$, (**d**) $[Zn(L)Br_2]$

sharp singlet at δ 3.85 ppm. The amino proton resonance was not detected due to the fast tautomeric equilibrium of the H atoms in the imine rings. The spectral pattern changes significantly in the complex due to the coordination. The unresolved imine protons of the free ligand changes to a broad singlet at ca. δ 13 ppm in the complexes. This supports the argument that coordination most probably occurs through two imine nitrogen atoms, causing inhibition of the fluxional behaviour of imidazole ring, which was also indicated by vibrational spectra.

No significant changes are observed for bridging CH_2 protons due to complexation. This may be taken as evidence that the sulphur atom is not playing any role in the coordination sphere. If the sulphur atom is coordinated to the metal ion, it should have caused significant changes on bridging CH_2 protons due to the formation of bicycle [4.4.0] octane, hence, forming two different geminal protons, which will exhibit two sharp doublets with large coupling constants, as observed for $[Pd(L)Cl_2]$ complex [14].

The two simple singlets of the benzene ring protons in the ligand change to three slightly broad singlets showing some downfield chemical shifts due to complex formation. Particularly the $[Zn(L)Cl_2]$ complex shows a strong downfield resonance as singlet at δ 8.29 ppm,. This downfield resonance is most probably caused by the strong intramolecular effect from an electronegative atom; in this case the chloride ion. We assign these resonances to the H(4, 4′) proton atoms in complexes [8, 25]. This strong intramolecular effect most possibly caused the broadness of the vibration in 300 cm^{-1} region in the case of the $[Zn(L)Cl_2]$ complex in the i.r. Since low electro-negativity of iodide compared with chloride and bromide ions, the corresponding iodide complex did not show this particular chemical shift.

The ^{13}C-n.m.r. spectrum of the benzimidazole moiety in the ligand, exhibits only four signals due to fast tautomeric equilibrium. Upon complexation, the fluxional behaviour of the imine proton is inhibited and the complexes exhibit eight signals including bridging aliphatic protons. The CH_2 resonance shifts from δ 29.00–25.17 ppm. in all three complexes. This up field resonance on CH_2 carbon, is most probably caused by shielding effect, either by the sulphur atom or imine groups or both. This shielding tends to support coordination via the nitrogen atoms instead of sulphur. The sulphur atom coordination will result in a strong de-shielding effect on this particular carbon atom, causing downfield resonances instead of up field, which is observed in all three complexes (see "Experimental"). Shifts were also observed in the complexes as compared with free ligand; particularly for C(2, 2′), C(4, 4′), C(8, 8′) and C(9, 9′) carbon atoms of the benzimidazole ring, giving strong support for coordination at the nitrogen atoms. A downfield resonance of one of these signal $\delta 115.17 \rightarrow 118.35$ ppm, may be caused by the strong intramolecular effect of an electronegative chloride and bromide ions, already suggested for H(4, 4′) hydrogen atoms. We assign this resonance to C(4, 4′) carbon atoms [14].

Conclusions

In conclusion, the analytical, vibrational, nuclear magnetic spectroscopic studies, and quantum chemical calculations on the ligand and complex prove that co-ordination occurs through two N(3, 3′) nitrogen atoms of imidazole units, together with the two anionic halide ligands to the metal centre, as a result forming four-coordinate tetrahedral complexes with the C_s symmetry.

Table 2 Experimental and computed vibrational frequencies (cm^{-1}) of $[Zn(L)Cl_2]$ with their assignment and TED values

No	Sy	IR	Raman	Scale[a]	TED (phases and %)[b]
Q1	A'	3313mb		3510	ν(N–H)(100)
Q2	A''			3509	ν(N–H)(100)
Q3	A'	3172s	3078	3107	ν(C–H)(100)
Q4	A''	3142s		3105	ν(C–H)(100)
Q5	A'	3123s		3094	ν(C–H)(100)
Q6	A''	3047sh		3084	ν(C–H)(100)
Q7	A'			3083	ν(C–H)(100)
Q8	A''			3073	ν(C–H)(100)
Q9	A'	2978w	2977	3017	$\nu(CH_2)$(100)
Q10	A''	2968w	2970	3014	$\nu(CH_2)$(100)
Q11	A'		2954	2962	$\nu(CH_2)$(100)
Q12	A''			2960	$\nu(CH_2)$(100)
Q13	A'	1623m	1623	1646	ν(6mr)(58), ν(5mr)(12), δ(CH)(11)
Q14	A''			1612	ν(6mr)(52), ν(CC)(20), δ(CH)(12)
Q15	A'			1611	ν(6mr)(52), ν(6mr)(14), ν(CC)(13), δ(NH)(13)
Q16	A''	1596w	1596m	1544	ν(5mr)(42), ν(CC)(20), δ(CH)(12)
Q17	A'			1539	ν(5mr)(39), δ(NH)(15), ν(6mr)(14), ν(CC)(13)
Q18	A''	1530wm	1529ms	1512	ν(6mr)(32), δ(CH)(26), ν(5mr)(23),δ(5mr)(12)
Q19	A'		1523ms	1510	ν(6mr)(32), δ(CH)(26), ν(5mr)(24),δ(5mr)(12)
Q20	A''	1485m	1486ms	1473	δ(CH)(40), ν(5mr)(22), ν(6mr) (14), ν(CC)(12)
Q21	A'			1471	δ(CH)(41), ν(5mr)(21), ν(6mr)(14) ν(CC)(14)
Q22	A'		1460sh	1467	$sc(CH_2)$(91)
Q23	A''	1452vs	1452vs	1454	$sc(CH_2)$(64), ν(5mr-CN)(30)
Q24	A''			1453	ν(5mr-CN)(29), δ(CH)(26)
Q25	A'	1421s	1421s	1447	$sc(CH_2)$(25), ν(5mr)(23), δ(CH)(19)
Q26	A''			1386	ν(6mr)(48), δ(CH)(18), ν(5mr)(11)
Q27	A'	1370mw	1368mb	1326	δ(CH)(42), ν(6mr)(21), ν(5mr)(16)
Q28	A'			1325	δ(CH)(41), ν(6mr)(21), ν(5mr)(17)
Q29	A''	1315s		1298	$\omega(CH_2)$(88)
Q30	A'	1279s	1278s	1287	ν(5mr)(36), δ(CH)(24), ν(6mr) (18)
Q31	A''			1285	ν(5mr)(35), δ(CH)(25), ν(6mr)(18)
Q32	A'		1254w	1271	$\omega(CH_2)$(90)
Q33	A''	1242m	1239mw	1241	δ(CH)(29), ν(5mr)(22), δ(NH)(19),ν(6mr)(16)
Q34	A'			1239	δ(CH)(29), ν(5mr)(23), δ(NH) (17),ν(6mr)(17)
Q35	A''	1231m	1229mw	1225	ν(5mr)(30), $t(CH_2)$(24), δ(6mr)(16), δ(NH)(12)
Q36	A'	1216ms	1216ms	1219	δ(CH)(45), ν(6mr)(34)
Q37	A''			1180	$T(CH_2)$(47), δ(NH)(20), ν(5mr)(15)
Q38	A'	1157s	1155s	1164	δ(CH)(76), ν(6mr)(16)
Q39	A''			1151	$T(CH_2)$(55), ν(5mr)(13), δ(NH)(12)
Q40	A'	1131vw	1131w	1128	δ(CH)(45), ν(6mr)(34)
Q41	A''			1127	δ(CH)(45), ν(6mr)(33)
Q42	A'	1048ms	1047s	1046	δ(5mr)(32), ν(5mr)(28), ν(6mr)(14), ν(CC)(12)
Q43	A''			1044	δ(5mr)(31), ν(5mr)(28), ν(6mr)(15), ν(CC)(11)
Q44	A'	1005ms	1005ms	1018	ν(6mr)(60), δ(CH)(19)
Q45	A'			1017	ν(6mr)(58), δ(CH)(18)
Q46	A''	950sh	974w	980	γ(C–H)(100)
Q47	A''			979	γ(C–H)(100)

Table 2 continued

No	Sy	IR	Raman	Scale[a]	TED (phases and %)[b]
Q48	*A′*	935w	934mw	933	γ(C–H)(100)
Q49	*A″*			932	γ(C–H)(100)
Q50	*A′*			927	$\rho(CH_2)$(46), δ(6mr)(25)
Q51	*A″*	911m	889mb	905	δ(6mr)(60), ν(5mr)(15)
Q52	*A′*			885	δ(6mr)(41), $\rho(CH_2)$(29), ν(5mr)(13), δ(5mr)(11)
Q53	*A″*	852ms	851vs	856	γ(C–H)(97)
Q54	*A′*			855	γ(C–H)(96)
Q55	*A″*			853	ν(6mr)(28), ν(CC)(23), ν(5mr)(16)
Q56	*A′*			852	ν(6mr)(26), ν(CC)(21), ν(5mr)(15)
Q57	*A′*			829	$\rho(CH_2)$(74)
Q58	*A″*	768sh	768vs	767	τ(6mr)(42), τ(5mr)(37), γ(C–H)(12)
Q59	*A′*			766	τ(6mr)(48), τ(5mr)(36), γ(C–H)(11)
Q60	*A″*			754	γ(C–H)(32), τ(5mr)(27), τ(6mr)(21)
Q61	*A″*	748vs	749vs	753	γ(C–H)(55), τ(5mr)(19), τ(6mr)(15)
Q62	*A′*			743	γ(C–H)(52), τ(5mr)(16)
Q63	*A″*	730sh	735w	739	τ(5mr)(31), γ(C–H)(30), τ(8mr)(14)
Q64	*A′*	703w	710w	708	ν(CS)(36), δ(6mr)(20), δ(5mr)(15), ν(CC)(12)
Q65	*A″*	665mw	622m	699	ν(CS)(26), δ(6mr)(24), δ(5mr)(19), ν(CC)(15)
Q66	*A′*	645mw		634	ν(CS)(32), τ(5mr)(24), δ(6mr)(20)
Q67	*A″*			628	δ(5mr)(38), δ(6mr)(36), ν(6mr)(20)
Q68	*A′*	609		626	δ(5mr)(39), δ(6mr)(35), ν(6mr)(21)
Q69	*A″*		622m	620	ν(CS)(45), τ(5mr)(20), δ(6mr)(13)
Q70	*A′*	600		575	τ(6mr)(78), τ(5mr)(22)
Q71	*A″*		518mw	517	δ(6mr)(35), γ(NH)(23)
Q72	*A″*			512	δ(6mr)(37), γ(NH)(19), ν(6mr)(12)
Q73	*A′*	488w	486m	489	γ(NH)(52), δ(6mr)(18), δ(ch-r)(12)
Q74	*A″*			487	γ(NH)(77)
Q75	*A′*			483	γ(NH)(30), δ(6mr)(23), δ(ch-r)(15), δ(5mr)(11)
Q76	*A′*			479	δ(6mr)(31), δ(ch-r)(20), δ(5mr)(14)
Q77	*A″*	438mw		437	τ(6mr)(67), but(CC)(13)
Q78	*A′*	363m	365mw	368	δ(ch-r)(37), τ(6mr)(18)
Q79	*A″*			348	τ(6mr)(36), δ(ch-r)(11)
Q80	*A′*			336	τ(ch-r)(37), τ(6mr)(16)
Q81	*A″*	320bsh	323	320	$\nu(ZnCl_2)$(93)
Q82	*A′*	bb		290	τ(ch-r)(39), δ(ch-r)(15), δ(6mr)(14)
Q83	*A″*	bb		288	τ(6mr)(51), τ(5mr)(24), τ(ch-r)(13)
Q84	*A′*	300vb	290	285	$\nu(ZnCl_2)$(93)
Q85	*A′*	275vb	251w	278	τ(6mr)(59), τ(5mr)(27)
Q86	*A″*	Bb		237	δ(ch-r)(41), ν(ZnN)(30)
Q87	*A′*		215	201	ν(ZnN)(29), τ(ch-r)(17), δ(ch-r)(11)
Q88	*A′*	197w	196mw	188	ν(ZnN)(24), δ(ch-r)(14), τ(ch-r)(14), but(CC)(13)
Q89	*A″*			176	ν(ZnN)(49), δ(ch-r)(17)
Q90	*A′*		147ms	144	τ(ch-r)(18), δ(8mr)(18), sc$(ZnCl_2)$(15), ν(ZnN)(14)
Q91	*A″*		118vs	134	Sc$(ZnCl_2)$(53), $\rho(ZnCl_2)$ (37)
Q92	*A′*			132	$\omega(ZnCl_2)$(67), δ(ch-r) (13), τ(ch-r)(12)
Q93	*A″*			124	δ(ch-r)(56), τ(ch-r)(22), sc $(ZnCl_2)$(17)
Q94	*A′*			110	δ(ch-r)(45), τ(ch-r)(20), $\omega(ZnCl_2)$(16)
Q95	*A″*			109	δ(ch-r)(39), $\rho(ZnCl_2)$(37)

Table 2 continued

No	Sy	IR	Raman	Scale[a]	TED (phases and %)[b]
Q96	A'			108	τ(ch-r)(39), $\rho(ZnCl_2)$(32), sc$(ZnCl_2)$(14)
Q97	A'		84vs	80	t$(ZnCl_2)$(70), but(C–N)(16)
Q98	A''			69	τ(ch-r)(65), τ(5mr)(16)
Q99	A'			60	τ(ch-r)(37), $(ZnCl_2)$(20), but(C–N)(16)
Q100	A'		38ms	43	τ(ch-r)(43), δ(ch-r)(17), t$(ZnCl_2)$(13)
Q101	A''			17	τ(ch-r)(46), δ(ch-r)(18), but(C–N)(18)

[a] Modes Q1–Q12 were scaled by 0.9620, Q13–Q70 by 0.980 and Q71–Q101 not scaled, see text

[b] Vibrational assignment is based on the calculated total energy distribution (TED). Only contributions over 10% are represented. ν, stretching; δ, in-plane bending; γ, out-of-plane bending; τ, torsion; ρ, rocking; t, twisting; ω, wagging, sc, scissoring; but, butterfly; m, medium; s, strong; v, very; w, weak; b, broad; sh, shoulder. ch-r, chelate-ring 8-membered

Acknowledgements We would like to thank Professor Peter Pulay for providing us with the SCALE 2.0 program and acknowledge the financial support from Fatih University.

References

1. Foster CJ, Kilmer CA, Thornton-Pett M, Halcrow MA (2002) Polyhedron 21:1031
2. Ismail MA, Brun R, Wenzler T, Tanious FA, Wilson WD, Boykin DW (2004) Bioorg Med Chem 12:5405
3. MacDonald LM, Armson A, Thompson RCA, Reynoldson JA (2004) Mol Biochem Parasitol 138:89
4. Agh-Atabay NM, Dulger B, Gucin F (2005) Eur J Med Chem 40:1096
5. Delescluse C, Piechock MP, Ledirac N, Hines RH, Li R, Gidrol X, Rahmani R (2001) Biochem Pharmacol 61:399
6. Monthilal KK, Karunakaran C, Rajendran A, Murugesan R (2004) J Inorg Biochem 98:322
7. Orjales A, Mosquera R, Toledo A, Pumar C, Labeaga L, Innerarity A (2002) Eur J Med Chem 37:721
8. Agh-Atabay NM, Dulger B, Gucin F (2003) Eur J Med Chem 38:875
9. Wang J, Li S, Xiao X, Zeng Y, Li Z, Matsumura-Inoue T (2005) J Inorg Biochem 99:883
10. Kasuga NC, Sekino K, Ishikawa M, Honda A, Yokoyama M, Nakano S, Shimada N, Koumo C, Nomiya K (2003) J Inorg Biochem 96:298
11. Matthews CJ, Leese TA, Clegg W, Elsegood MRJ, Horsburgh L, Lockhart JC (1996) Inorg Chem 35:7563
12. Matthews CJ, Clegg W, Heath SL, Martin NC, Stuart Hill MN, Lockhart JC (1998) Inorg. Chem 37:199–207
13. Matthews CJ, Leese TA, Thorp D, Lockhart JC (1998) J Chem Soc Dalton Trans 79–88
14. Agh-Atabay NM, Baykal A, Somer M (2004) Trans Met Chem 29:159
15. Addison AW, Burke PJ (1981) J Heterocycl Chem 18:803
16. Berends HP, Stephan DW (1984) Inorg Chim Acta 93:173–178
17. Frisch MJ, Trucks GW, Schlegel HB, Scuseria GE, Robb MA, Cheeseman JR, Montgomery JA, Vreven T Jr, Kudin KN, Burant JC, Millam JM, Iyengar SS, Tomasi J, Barone V, Mennucci B, Cossi M, Scalmani G, Rega N, Petersson GA, Nakatsuji H, Hada M, Ehara M, Toyota K, Fukuda R, Hasegawa J, Ishida M, Nakajima T, Honda Y, Kitao O, Nakai H, Klene M, Li X, Knox JE, Hratchian HP, Cross JB,, Bakken V, Adamo C, Jaramillo J, Gomperts R, Stratmann RE, Yazyev O, Austin AJ, Cammi R, Pomelli C, Ochterski JW, Ayala PY, Morokuma K, Voth GA, Salvador P, Dannenberg JJ, Zakrzewski VG, Dapprich S, Daniels AD, Strain MC, Farkas O, Malick DK, Rabuck AD, Raghavachari K, Foresman JB, Ortiz JV, Cui Q, Baboul AG, Clifford S, Cioslowski J, Stefanov BB, Liu G, Liashenko A, Piskorz P, Komaromi I, Martin RL, Fox DJ, Keith T, Al-Laham MA, Peng CY, Nanayakkara A, Challacombe M, Gill PMW, Johnson B, Chen W, Wong MW, Gonzalez MW, Pople JA (2004) Gaussian 03, Revision C.02. Gaussian, Inc., Wallingford, CT
18. Pongor G (1977) SCALE2. Eotvos University, Budapest
19. Pulay P, Fogarasi G, Pang F, Boggs JE (1979) J Am Chem Soc 101:2550
20. Scott AP, Radom L (1996) J Phys Chem 100:16502
21. Palafox MA (2000) Int J Quant Chem 77:66
22. National Institute of Technology, NIST Standard Reference Database 2005
23. Ellis RB (1966) J Electrochem Soc 113:485
24. El-Akhras Z (1977) Dissertation Technical University Clausthal
25. Nakamoto K (1997) Infrared, Raman spectra of inorganic coordination compounds, Part B, 5th edn., Wiley, p 38
26. Van der Poel H, Van Koten G, Vrieze K (1980) Inorg Chem 19:1145
27. Siebert H (1966) Anwendungen der Schwingungsspektroskopie in der Anorganischen Chemie, Springer Verlag, Berlin, p 66
28. Avery JS, Burbridge CD, Goodgame DML (1968) Spectrochim Acta 24A:1721
29. Thornton DA (1990) Coord Chem. Rev 104:251
30. Demertzi D, Nicholls D (1983) Inorg Chim Acta 73:37
31. Akyüz S, Davis JED, Dempster AB, Holmes KT (1976) J Chem Soc Dalton Trans 1746
32. Ferraro JR (1971) Low frequency vibrations of inorganic and coordination compounds. Plenum Press, New York